Pharmaceutical Research, Vol. 7, No. 3, 1990

Research Article

Transport Mechanisms in Iontophoresis. II. Electroosmotic Flow and Transference Number Measurements for Hairless Mouse Skin[1]

Michael J. Pikal[2,3] and Saroj Shah[2]

Received March 20, 1989; accepted August 1, 1989

Previous studies suggest that bulk fluid flow by electroosmosis is a significant factor in iontophoresis and may provide an explanation for the observed enhanced transport of neutral species. In a charged membrane, the solution carries a net charge and thus experiences a volume force in an electric field, which causes volume flow (J_v) in the direction of counterion flow. J_v data were obtained for hairless mouse skin (HMS) as a function of pH, concentration of NaCl, current density, and time. Volume flow was measured by timing fluid movement in horizontal capillary tubes attached to the anode and cathode (Ag/AgCl) compartments. By convention, the sign of J_v is taken as positive when the volume flow is in the same direction as positive current flow. Experimental mean values were in the range 0 to +37 μl/cm² hr, depending on the experimental conditions. Volume flow of this magnitude is large enough to have significant impact on flow of both ions and neutral species. The positive sign for J_v indicates that HMS is negative in the pH range studied (3.8–8.3). J_v decrease with time, decrease with increasing NaCl concentration, are much lower at pH 3.8 than at the higher pH's, and increase with current density. Effective transference numbers, determined from membrane potential measurements, showed significant pH dependence, consistent with a small negative charge on the membrane at mid pH's and charge reversal around pH 4. Both electrical resistance and J_v data indicate changes in transport properties occur when HMS is subjected to an electric field.

KEY WORDS: transdermal; iontophoresis; electroosmosis; volume flow; transference number; electrical resistance.

INTRODUCTION

In the first paper in this series (1), a theoretical analysis was employed to demonstrate that volume flow via electroosmosis can be an important factor in flux enhancement by iontophoresis. In this paper, the experimental foundation of the preceding theoretical analysis is presented. Specifically, volume flow data and related supplementary data for hairless mouse skin (HMS) are presented.

Bulk fluid flow or volume flow occurs in the direction of counterion migration when an electrical potential difference is applied across a "porous" membrane containing fixed charges (i.e., ionic groups immobilized in the membrane) (2–4). This volume flow is referred to as electroosmotic flow. Under conditions of equal temperature, pressure, and fluid composition on both sides of the membrane, a potential gradient, $-d\phi/dx$, produces electroosmotic volume flow, J_v (units of volume time^{-1} area^{-1}), in direct proportion to the potential gradient,

$$J_v = L_{VE}(-d\phi/dx) \quad (1)$$

where L_{VE} is the electroosmotic flow coefficient. Note that the sign convention gives positive volume flow when the counterions are positive (i.e., the membrane is negative). Volume flow will enhance or retard the flux of the solute of interest, ionic or neutral, depending on whether the flux of interest is with or against the volume flow "stream."

In 1924, Rein (5) reported the results of a series of investigations on volume flow across excised human skin. Rein measured flows equivalent to J_v values of ≈100 μl hr^{-1} cm^{-2} in water at neutral pH and current densities of 1 mA/cm². Note that, assuming a solute moves with the solvent, a volume flow of 100 μl hr^{-1} cm^{-2} is equivalent to delivery of 2 mg hr^{-1} cm^{-2} from an external solution of 20 mg/ml. The addition of NaCl appeared to decrease J_v, but because of lack of reproducibility, this conclusion is uncertain. At pH 3, J_v was essentially zero. At pH values less than 3, transient negative J_v values were observed. Thus, the data indicate that above pH ≈ 3, human skin is negatively charged, and below pH ≈ 3, human skin is weakly positively charged.

The main objective of this research was to obtain quantitative volume flow data on hairless mouse skin to allow a more quantitative interpretation of the role of volume flow in iontophoresis studies. Volume flow data were obtained as a function of pH, NaCl concentration, and current density.

[1] Presented, in part, at the 1st National Meeting of the AAPS, Washington, D.C., November 1986.

[2] Lilly Research Laboratories, Eli Lilly & Co., Indianapolis, Indiana 46285.

[3] To whom correspondence should be addressed.

0724-8741/90/0300-0213$06.00/0

Electrical resistance data were measured by a DC technique to aid in the interpretation of the volume flow data, and transference numbers of Cl^- were measured as a function of pH at several NaCl concentrations in an attempt to characterize the electrical charge of the skin as a function of pH.

EXPERIMENTAL

Materials

All chemicals were reagent grade, and the water was water for injection (Eli Lilly & Co.). Adjustment of solution pH was made by addition of small quantities of HCl or NaOH. A pH measurement was made after an experiment to ensure that excessive pH drift had not occurred. The ion-exchange membranes used as "control" membranes in the volume flow and transference number measurements were obtained from Ionac. The cation exchange membrane (No. 61 CZL 386) was a sulfonic acid type, and the anion exchange membrane (No. 204 SXZL 386) was a tertiary amine type. Both ion-exchange membranes are 0.6 mm in thickness, have area specific resistances of $\approx$10 Ω-cm^2 in 0.1 *M* NaCl, counterion transference numbers of $\approx$0.95 in dilute NaCl, and a high exchange capacity (3–4 Eq/kg H_2O). The skin was full-thickness dorsal hairless mouse skin (HRS/J, Jackson Labs, 1 to 6 month-old female), which was removed after sacrifice by cervical dislocation. The skin sample was equilibrated prior to use by soaking in the solution of interest. In the EMF transference number experiments, equilibration was with the more concentrated solution. The equilibration procedure was either about 2 hr at room temperature or overnight at $\approx$5°C, followed by warming to room temperature. While there were no systematic difference in J_v results when the two equilibration procedures were compared, the overnight procedure seemed to yield more rapid stabilization in the electroosmotic flow experiment and therefore was used for most of the later J_v experiments (NaCl concentrations greater than 0.05 *M*). Room temperature equilibration was used for all other experiments.

Apparatus and Procedures

Volume Flow Measurements. The cell design (Fig. 1) was a modification of the design used by Kobatake and coworkers (4). The skin (or ion-exchange membrane) was sandwiched between two stainless-steel plates (0.75-mm thickness) perforated with numerous 1-mm-diameter holes. The steel plates prevent volume changes which would result from deformation of the skin during the experiment yet allows the entire skin or membrane area (3.1 cm^2) to be available for transport.[4] The steel plates and skin were clamped between the two large "O-ring" joints of the half cells with a nylon clamp assembly. The O-ring and both joints were lightly coated with high-vacuum silicone stopcock grease to ensure a leak tight seal. The disk-shaped electrodes were

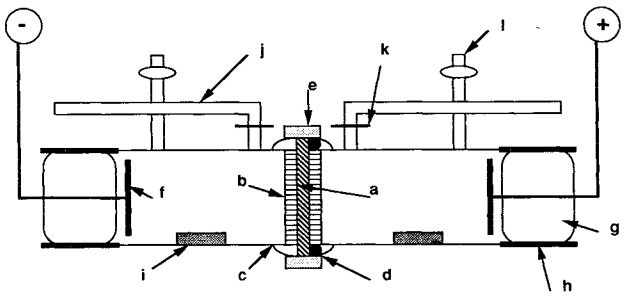

Fig. 1. Schematic of electroosmotic flow cell. Total volume = 120 ml. (a) Skin; (b) 1-mm-thick stainless-steel plate with 1-mm-diameter holes; (c) No. 20 "O"-ring joints; (d) Viton O-ring on stratum corneum side; (e) nylon clamp; (f) Ag/AgCl electrodes; (g) 34/28 inner standard taper joint containing electrodes; (h) 34/28 outer standard taper joint; (i) magnetic stirring bars; (j) 1-mm-diameter capillary tubes; (k) No. 5 O-ring joint to attach capillary tubes; (l) filling tubes.

sealed into the glass of "inner" standard taper joints, which then fit into the "outer" standard taper joint attached to the body of each half cell. The electrodes were Ag/AgCl electrodes prepared by thermal decomposition of silver oxide which had been coated on a silver disk, followed by chloridization in HCl (6). Magnetic stirring bars driven by water pressure operated stirring mechanisms located underneath the open plexiglas water bath (not shown) into which the assembled volume flow cell was placed. Two horizontal precision 1-mm ($\pm$0.01-mm)-diameter capillary tubes were attached via O-ring joints. Filling tubes with stopcocks were provided to aid in filling the cell completely without leaving air bubbles. All solutions were degassed by warming ($\approx$37°C) under vacuum and filled immediately to avoid bubble formation. After filling, the cell was placed in the water thermostat at 35°C (stable within $\pm$0.05°C), which in turn was in an air thermostat operating at 35 $\pm$ 0.5°C. This arrangement assured that even the capillary tubes, which were above the water level in the bath, were temperature controlled. After thermal equilibration, solution was added to each half-cell through the filling tubes such that the position of the solution meniscus in each capillary tube was appropriate for the volume flow experiment. The position of each meniscus (i.e., in capillary tubes attached to both dermis and stratum corneum sides of the cell) was then monitored as a function of time using a cathetometer (Eberbach, Ann Arbor, Michigan). Normally within an hour, the system would stabilize in the sense that movement of the meniscus would be minimal. The experiment would then be started by recording the position of each meniscus as a function of time for 20–30 min to establish a "blank" volume flow under conditions of zero current flow (Fig. 2A). Next, the current would be turned on (General Resistance Model E-35 constant-current source) such that the stratum corneum was facing the anode, and the position of each meniscus would be measured as a function of time (Fig. 2B). The current would then be turned off, and an additional "blank" volume flow data set would be taken (Fig. 2C). In most experiments, the second blank would be followed by data collection with the same magnitude of current flow but with the polarity reversed (i.e., dermis facing the anode) (Fig. 2D). Slopes of each of the position-vs-time curves were determined by linear regression, and the electroosmotic flow rate, J_v, was

[4] Due to rigidity of the ion-exchange membranes provided by embedded fiber, J_v data for ion-exchange membranes could be obtained with or without the use of the steel plates. The use of plates did not cause a significant difference in J_v. Moreover, the electrical resistance of hairless mouse skin appeared to be at least roughly independent of the use of plates (see Figs. 3 and 4).

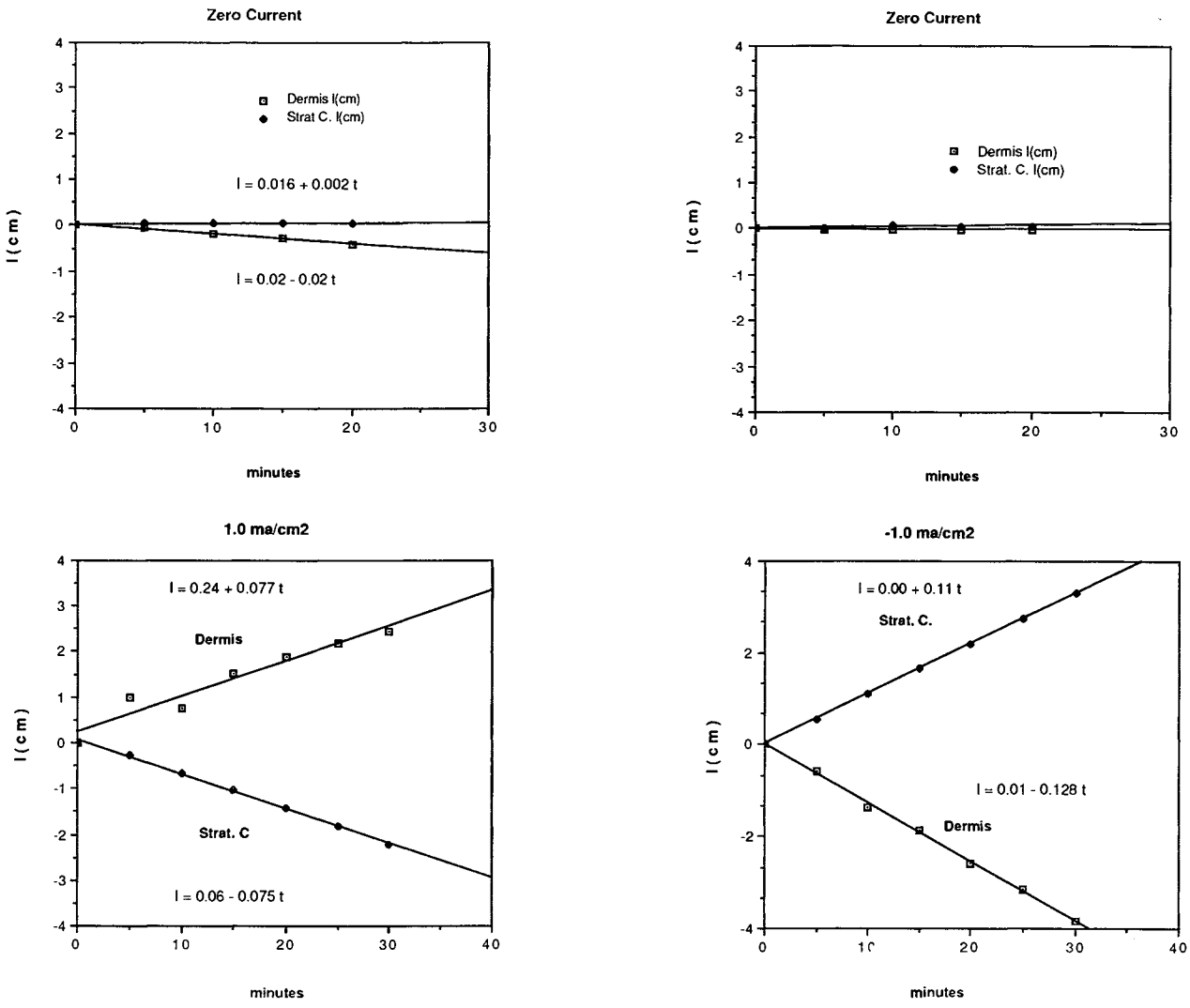

Fig. 2. Typical electroosmotic flow experiment. Each panel shows displacement of the meniscus in the capillary tubes (dermis and stratum corneum sides) as a function of time. The sequence of the experiment is zero current (top left panel), normal polarity or "positive current" (bottom left), zero current (top right), and reverse polarity or "negative current" (bottom right).

calculated from the product of the cross-sectional area of the capillary tube and the linear flow rate, *dl/dt*, corrected for the blank effect. The mean of the first blank (Fig. 2A) and second blank (Fig. 2C) was used to correct the flow rate for the "positive current" run (Fig. 2B), while the second blank is used to correct the reverse polarity data (Fig. 2D). Note that 4 cm of linear movement corresponds to a volume of only 30 μl.

All volume flow experiments at 1 mA/cm^2 started with skin not previously exposed to current flow. Most of the 2-mA/cm^2 experiments used the same skin sample that previously was used to generate the volume flow data at 1 mA/cm^2. Several volume flow experiments at 2 mA/cm^2 (pH 5.8) were also run using skin not previously exposed to current flow. The resulting J_v data appeared independent of this variation in procedure.

Electrical Resistance Measurements. Electrical resistance measurements on hairless mouse skin were made using a DC method (7). The capillary tubes on the volume flow apparatus (Fig. 1) were replaced by Small Ag/AgCl "probe" electrodes. These electrodes were prepared as described earlier except that the support for the silver oxide was a spiral of platinum wire. Constant current was passed through the cell, and the potential drop (voltage) between the two probe electrodes was measured with a voltmeter (Fluke, Model 8020B). The current was reversed, and the potential drop was again measured. The difference between the two voltages, with due consideration for sign, was divided by twice the current to yield the total resistance for the circuit composed of the skin and solution between the skin and electrodes. This procedure eliminates error due to bias potential in the electrodes (7). The skin resistance was then obtained by subtracting the solution resistance, measured in a separate experiment, from the total resistance.

Transference Numbers. Transference numbers were determined by a variation of the EMF method (3,8) where voltage measurements (EMF) of electrochemical cells of the type indicated in Scheme 1.

$$Hg/Hg_2Cl_2(s)/KCl(satd):NaCl(m_2)//membrane//NaCl(m_1):KCl(satd)/HgCl_2(s)/Hg$$

Scheme 1

may be used to evaluate a mean transference number of the sodium ion, t_{Na^+},

$$t_{Na^+} = F\,EMF/2RT\ln[(m\,\gamma_\pm)_2/(m\,\gamma_\pm)_1] + 0.5; \quad t_{Na^+} + t_{Cl^-} = 1.00 \qquad (2)$$

where F is Faraday's constant, R is the gas constant, T is the absolute temperature, $\gamma_\pm$ is the mean ionic activity coefficient for NaCl solution of molality m_1 or m_2 ($m_2 > m_1$), and EMF is the electromotive force (voltage) of the cell. The EMF of the above cell is positive (i.e., the dilute solution *is* the cathode side) if $t_{Na^+} > 0.5$. The electrodes were calomel electrodes with a porous ceramic plug serving as the salt bridge (Corning No. 476242).[5] The two half-cells of a conventional transdermal diffusion cell (Valia-Chien, Crown Glass) were filled with solutions at concentrations m_1 and m_2, allowed to equilibrate for about 0.5 hr, emptied, and refilled with fresh solution. The electrodes were attached to both compartments via adapters, and the EMF was then measured periodically with a digital voltmeter (Orion model No. 501, Ionalyzer) until a stable reading was obtained (usually 0.5 to 1 hr).

The use of Eq. (2) makes the usual assumption that the diffusion potential at the KCl salt bridge (denoted by a colon in Scheme 1) is essentially zero and also assumes that essentially all the current is transported by NaCl. The transference number is a mean transference number in the membrane and therefore refers to a mean external NaCl concentration of $(m_1 + m_2)/2$. In our experiments, the ratio m_2/m_1 was always 2.0. In principle, there is a correction to the transference number calculated from Eq. (2), which involves volume flow of solvent (9). This correction is less than our experimental error and, therefore, is ignored. Activity coefficient data, $\gamma_\pm$, were taken from the literature (10). As a check on accuracy of the method, EMF transference numbers for NaCl in aqueous solution were determined using concentration cells, where the liquid–liquid junction between two NaCl solutions is formed in a stopcock (11). Agreement with the literature (12) was within ±0.01 in transference number. The Hittorf method (8) was used to measure transference numbers of Na^+ and Cl^- in HMS (pH 6, 0.05 *M* NaCl, 1.6 mA/cm^2 for 3 hr) with the results $t_{Na^+} = 0.33 \pm 0.02$ and $t_{Cl^-} = 0.65 \pm 0.03$. The corresponding interpolated EMF result, $t_{Na^+} = 0.39 \pm 0.04$, is in satisfactory agreement. The Hittorf method could not be used at low pH due to severe skin damage (i.e., holes) developing during the experiment. For example, an overnight experiment (pH 4, 1.6 mA/cm^2) produced a hole in the skin about 4 mm in diameter.

[5] We also explored the use of Ag/AgCl electrodes in a cell similar to that shown in Scheme 1 but without the KCl salt bridge (3,8). From a purist viewpoint, such a cell is superior to Scheme 1 since the assumption of zero diffusion potential at the salt bridge does not arise. These cells without the salt bridge were used to determine the transference numbers for the ion-exchange membranes studied. Transference numbers for hairless mouse skin at pH 7 and 0.038 M NaCl were also determined without difficulty (mean $t_{Cl^-} = 0.56 \pm 0.03$; compared to the mean evaluated using the cell in scheme 1, $t_{Cl^-} = 0.58 \pm 0.04$). However, at low pH, stable and reproducible EMFs could not be obtained with the Ag/AgCl cells. The problem was traced to a component of unknown composition leaching from the skin at low pH which interferes with the electrode reaction. Since the calomel electrodes in Scheme 1 are isolated from the solution containing the contaminant by the salt bridge, the interference problem does not arise.

RESULTS

DC Electrical Resistance

Figure 3 shows the time dependence of the electrical resistance of hairless mouse skin in 0.05 *M* NaCl (pH 6) during iontophoresis at 1.6 mA/cm^2. At selected times, iontophoresis was briefly interrupted, and the DC electrical resistance was determined at current densities of 0.032, 0.32, and 1.6 mA/cm^2 (skin sample A) and at 1.6 mA/cm^2 only for skin sample B. The initial resistance for 0.032 mA/cm^2 is off the scale of the plot (13.7 kΩ-cm^2). The resistance for sample B at 22 hr (not shown) is 0.52 kΩ-cm^2, about a 28% decrease over the 6 to 22 hr time period. The lines connecting the points have no theoretical significance and may not accurately represent details of the time dependence between the first two time points.

The effect of current density and pH on the resistance of hairless mouse skin in 0.05 *M* NaCl is illustrated by Fig. 4. The resistance measurements were made after the conclusion of a volume flow experiment run (see Fig. 2). The top graph (Fig. 4A) shows the variation in resistance with current density observed with two skin samples. While the data show variation in resistance between skin samples, both samples exhibit a linear decrease in resistance as the current density increases (mean decrease of ≈25% between 1 and 2 mA/cm^2). The bottom graph (Fig. 4B) gives mean data from a number of skin samples. Although resistance variation between skin samples somewhat obscures the current depen-

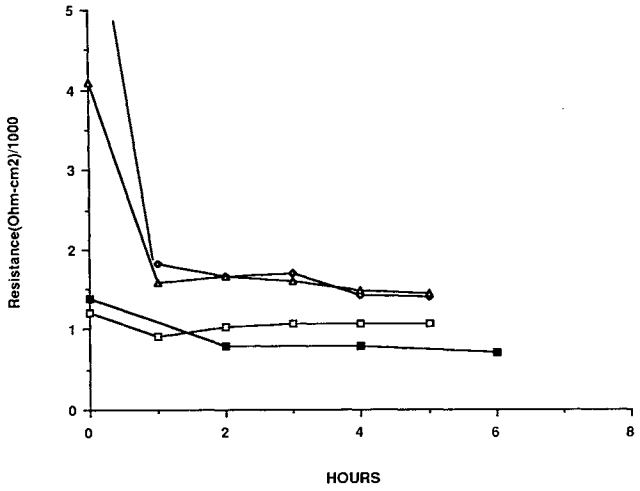

Fig. 3. The DC electrical resistance of hairless mouse skin at selected current densities as a function of time at 1.6 mA/cm^2. The skin was in contact with 0.05 *M* NaCl (pH 6) at 35°C. Measurements made without using stainless-steel plates. Open symbols are skin sample A, and filled symbols are skin sample B. ◇, 0.032 mA/cm^2; △, 0.32 mA/cm^2; □ and ■, 1.6 mA/cm^2.

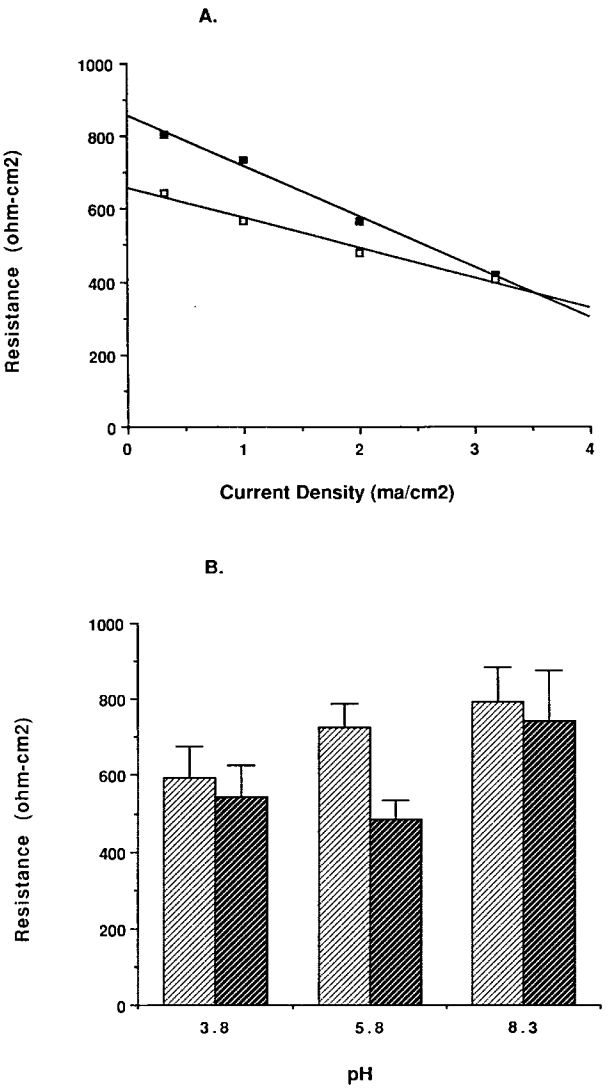

Fig. 4. The DC electrical resistance of hairless mouse skin as a function of current density and pH. Resistance measurements made (using stainless-steel plates) after an electroosmotic flow experiment. The skin was in contact with 0.05 *M* NaCl at 35°C. (A) Current density dependence with individual skin samples at pH 5.8; ■, skin sample 178; □, skin sample 182. (B) Mean values for various skin samples at 1 mA/cm^2 (light texture) and at 2 mA/cm^2 (dark texture). Number of replicates ranged from two to five.

dence, the resistance measured at 2 mA/cm^2 was always less than the resistance measured at 1 mA/cm^2 (mean decrease of ≈15% between 1 and 2 mA/cm^2). There also appears to be a slight trend of increasing resistance with increasing pH, although none of the differences are statistically significant even at the 90% confidence level. Additional data (not shown)[6] demonstrates that the skin resistance decreases as the concentration of NaCl increases, the reciprocal of resistance increasing roughly linearly with NaCl concentration.

[6] Data obtained at 1 mA/cm^2 after a volume flow experiment are as follows: (a) pH 5.8—728 ± 57 (0.05 *M*), 201 ± 6 (0.5 *M*); (b) pH 8.3—791 ± 90 (0.05 *M*), 710 ± 90 (0.1 *M*), 418 ± 48 (0.25 *M*), 214 ± 27 (0.5 *M*).

Volume Flow

Volume flow at neutral and slightly alkaline pH is essentially constant over the 0.5-hr time period used in the typical experiment to determine the initial volume flow, J_v (i.e., a plot of meniscus position vs time is linear; see Fig. 2). However, over longer periods of time, a reproducible decrease in J_v with time was observed (Table I). The 1- and 2-hr data at pH 5.8 (Table I) were generated by regression analysis on 0.5-hr segments of the meniscus position-vs-time curve. The mathematical relationship between J_v and time (Table I, footnote *a*) is strictly empirical. The standard errors give the impression that the mean J_v values between the 1-hr and the 2-hr time points are not significantly different. However, most of the standard error originates from a systematic difference in J_v between the skin samples. The ratio, J_v(2 hr)/J_v(1 hr), is 0.86 with a standard error of ±0.04. The time dependence at pH 3.8 is much more extreme, particularly at 2 mA/cm^2. Here, the data were generated by regression analysis on 15-min segments of the meniscus position-vs-time curves. Although the absolute reproducibility between samples was poor, J_v measured with 1.0 mA/cm^2 was always positive at time zero—with two of the five skin samples showing significant decreases in J_v after about 15 min of current flow. At a current density of 2.0 mA/cm^2, one of the samples gave a negative J_v at time zero which remained relatively constant with time. The other four samples gave positive J_v values at time zero. J_v was roughly constant for two of these samples, but the other two samples gave large negative J_v at the 0.38-hr time point. A negative value of J_v means simply that the volume flow is from cathode to anode, indicating that the membrane charge is positive. Thus, the volume flow at low pH shows significant variation between skin samples with frequent examples of negative volume flow. While negative volume flow of even greater magnitude may have been observed had the duration of the pH 3.8 experiments been longer, long runs at low pH run the risk of

Table I. Time Dependence of Volume Flow Through Hairless Mouse Skin at 35°C in 0.05 *M* NaCl: Anode on Stratum Corneum Side

No. of Runs	Time (hr)	J_v (μl/hr cm^2 ± SE)
	pH 5.8; current density, 1.0 mA/cm^2[a]	
7	0.0	11.2 ± 0.8
3	1.0	7.2 ± 1.0
3	2.0	6.2 ± 1.0
	pH 3.8; current density, 1.0 mA/cm^2	
5	0.0	8.2 ± 1.8[b]
5	0.38	3.6 ± 1.6[c]
	pH 3.8; current density, 2.0 mA/cm^2	
5	0.0	3.9 ± 4.0[d]
5	0.38	0.0 ± 3.0[e]

[a] Data well represented by $J_v = 11.2 \exp(-0.422\ t^{1/2})$, $R = -0.9991$.
[b] Range, 3.3 to 13.0; two of five samples show a sharp decrease after about 15 min.
[c] Range, −0.6 to +8.5.
[d] Range, −10.0 to +15.0.
[e] Range, −10.0 to +5.8.

severe skin damage. Although current flow at pH 3.8 obviously produced changes in J_v, these changes were not a result of holes in the skin. Skin resistance measurements made after the volume flow experiments at pH 3.8 are comparable to those made after measurements at pH 5.8 (Fig. 4B).

Volume flow in hairless mouse skin is compared to volume flow in cation and anion exchange membranes in Fig. 5, and the effect of pH on volume flow in hairless mouse skin is shown in Fig. 6. The light textured bars refer to measurements made at 1 mA/cm^2, while the darker texture refers to 2 mA/cm^2. Since the anion-exchange membrane is positively charged, the counterions are negative and flow from cathode to anode, thereby producing a negative volume flow. Both the cation-exchange membrane and hairless mouse skin produce positive volume flow. With ion-exchange membranes, the same value of J_v is obtained when the polarity on the volume flow cell is reversed, as expected. However, with hairless mouse skin, reversal of polarity places the anode on the dermis side of the skin sample, resulting in a significantly larger J_v than when the anode faces the stratum corneum. The data in Figs. 5 and 6 refer to measurements with 0.05 *M* NaCl in contact with the membranes. Variation in J_v with variation in concentration of NaCl is shown in Fig. 7. Error bars give the standard error in the mean when the error bar is larger than the plotting symbol. Experimental values of the electroosmotic flow coefficient, L_{ve}, were calculated from the J_v data and corresponding resistance data[6] using the analog of Eq. (1),

$$L_{ve} = J_v/(iR')$$

where J_v has units of μl/hr cm^2, i is the current density in amperes/cm^2, and R' is the area normalized resistance[6] in Ω-cm^2. Note that if consistent units are used and flux is

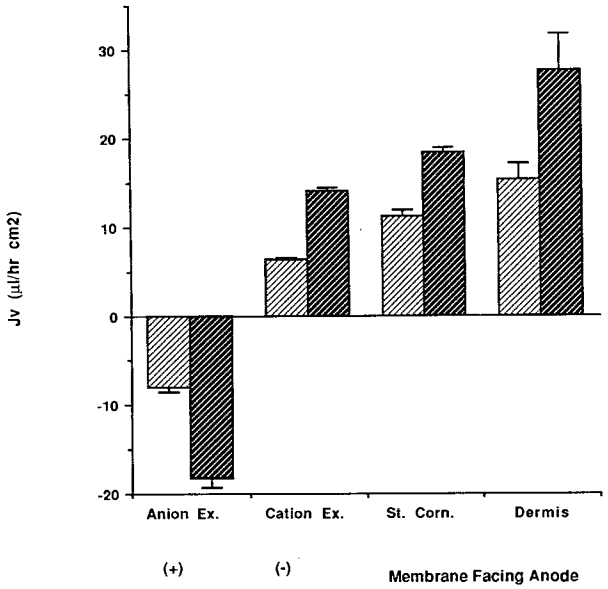

Fig. 5. The effect of membrane on initial electroosmotic volume flow: a comparison of hairless mouse skin with cation- and anion-exchange membranes. All solutions are 0.05 *M* NaCl at 35°C and pH 5.8. The light texture is 1.0 mA/cm^2, and the dark texture is 2.0 mA/cm^2.

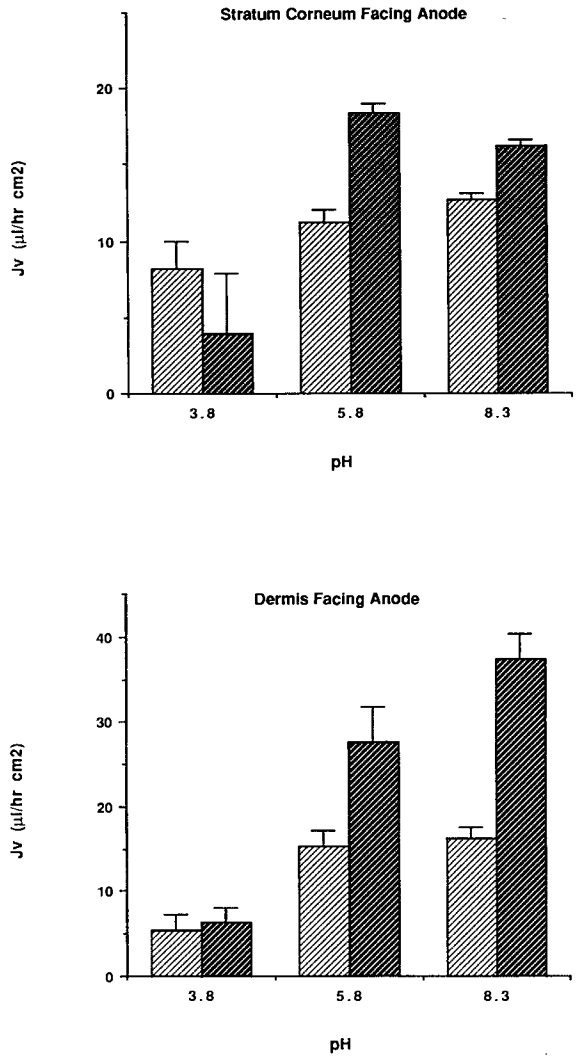

Fig. 6. The effect of pH on initial electroosmotic volume flow. All solutions are 0.05 *M* NaCl at 35°C and pH 5.8. The light texture is 1.0 mA/cm^2, and the dark texture is 2.0 mA/cm^2.

normalized to unit membrane area, the "experimental" coefficient, L_{ve}, is related to the coefficient in Eq. (1), L_{VE}, by the relation, $L_{ve} = L_{VE}/L$, where L is the thickness of the transport barrier. The variation of L_{ve} with concentration of NaCl is shown in Fig. 8. The sizable standard errors are a reflection mainly of the uncertainty in the resistance data.[6] The smooth curve is the result of a fit of the data to the theoretical result for L_{ve} (1). Since only one point (0.25 *M*) deviates from the theoretical curve by significantly more than the standard error, the agreement is probably within experimental error.

Transference Numbers

Transference numbers for chloride ion in hairless mouse skin as a function of pH are compared with corresponding data for ion-exchange membranes and aqueous NaCl solutions in Fig. 9. The open squares refer to hairless mouse skin data at a NaCl concentration of 0.038 *M*, while the filled squares are corresponding data at a NaCl concentration of

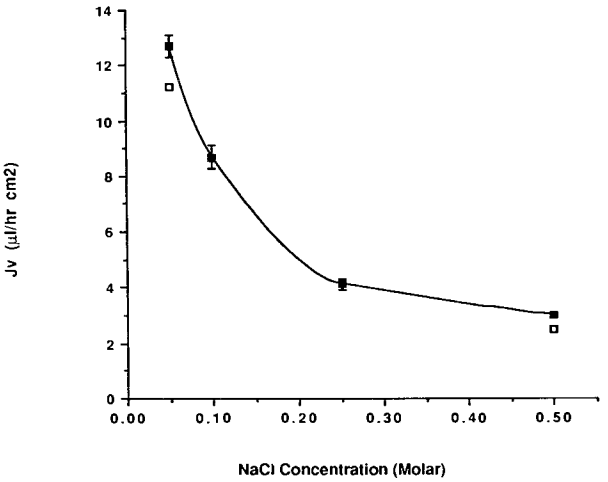

Fig. 7. The effect of NaCl concentration on initial electroosmotic volume flow at 35°C. The current density is 1.0 mA/cm^2 with the stratum corneum facing the anode. The filled squares are pH 8.3, and the open squares are pH 5.8.

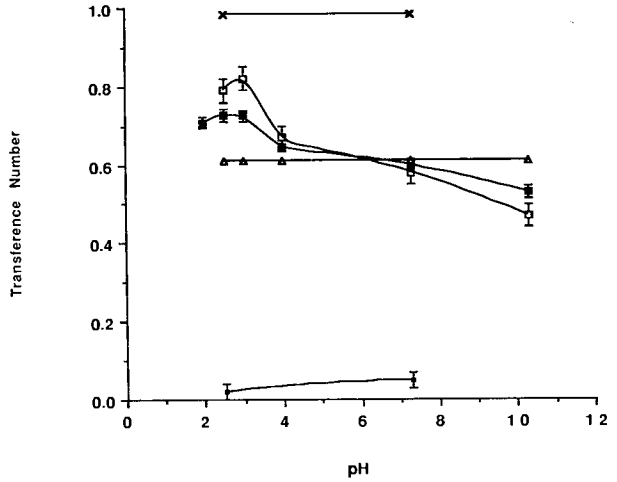

Fig. 9. Transference numbers of chloride ion in hairless mouse skin at 22°C as a function of pH: comparison with ion-exchange membranes and aqueous solution. □, hairless mouse skin, 0.038 *M* NaCl; ■, hairless mouse skin, 0.38 *M* NaCl; △, aqueous NaCl solutions, 0.038 and 0.38 M; x, anion-exchange membrane, 0.038 *M* NaCl; •, cation-exchange membrane, 0.038 *M* NaCl.

0.38 *M*. The triangles represent data for aqueous NaCl solutions at both 0.038 and 0.38 *M*, as the transference numbers for both concentrations were identical (±0.01). Transference number data given for cation-exchange membranes (negatively charged) and anion-exchange membranes (positively charged) refer to 0.038 *M* NaCl. Other data (not shown) indicate that higher NaCl concentrations decrease slightly the counterion transference numbers in ion-exchange membranes. Note that no buffers were used, so the solutions contain only NaCl, hydrogen ion, and hydroxide ion. Error bars are given when the error bars are larger than the plotting symbol. The lines drawn simply connect the data points and may not accurately predict transference number variation between data points.

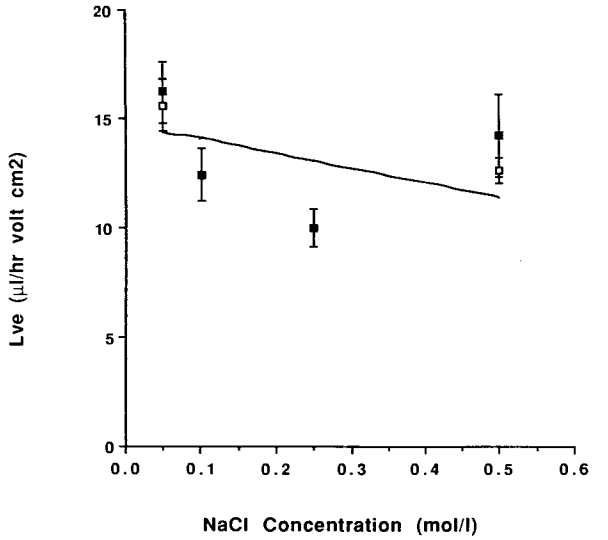

Fig. 8. The effect of NaCl concentration on the electroosmotic flow transport coefficient, L_{ve}, at 35°C. L_{ve} is evaluated from initial electroosmotic volume flow data, J_v, and the corresponding DC resistance measured after the volume flow experiment. The filled squares are pH 8.3, and the open squares are pH 5.8.

DISCUSSION

The resistances measured in this research are significantly lower than those determined by Burnette and Bagniefski for HMS (17). However, differences in procedure make a quantitative comparison difficult. Our procedure starts with a skin sample that is essentially fully hydrated (rather than partially hydrated), and prior exposure to current in this research refers to currents in the range of 1–2 mA/cm^2 (rather than 0.16 mA/cm^2). Moreover, measurement of resistance in this research is made at current densities in the range of 0.032 to 3.2 mA/cm^2 (rather than 1 µA/cm^2). The closest comparison is that for hydrated HMS (3 hr) with no prior exposure to current. Our result measured at 32 µA/cm^2 *for one skin sample* is 14 kΩ-cm^2, compared to 27 kΩ-cm^2 measured at 1 µA/cm^2 (17). Data from Fig. 4 indicate that for fully hydrated HMS previously exposed to current (1–2 mA/cm^2 for ≈1 hr), the resistance extrapolated to zero current density is ≈0.8 kΩ-cm^2, compared to a resistance of 6 kΩ-cm^2 measured at 1 µA/cm^2 after exposure to a current density of 0.16 mA/cm^2 for 1 hr (17). Thus, it would appear that the reduction of resistance upon passage of current depends on the current density.

Initial volume flow, J_v, in HMS was positive at all pH's studied, meaning that electroosmotic flow moved in the same direction as flow of positive ions. This observation is direct evidence (1) that the fixed charges lining "pores" in HMS, as in human skin (5), are predominantly negatively charged between pH 3.8 and pH 8.3. While J_v in HMS is of the same magnitude as J_v in the ion-exchange membranes, this observation does *not* imply the charge densities in the two membranes are comparable. At a given current density, J_v is roughly proportional to charge density only at a low charge density (1). J_v also depends roughly on the square of

the pore radius. The ion-exchange membrane data are consistent with theory (1) and the known charge concentration of ≈3.5 *M* if the pore radius is taken to be 4.5 Å, which is reasonable for ion exchangers (3) but much smaller than the ≈20 Å found for HMS (1). The slight increase in J_v for HMS with increasing pH (Fig. 6) suggests that any increase in charge density with increasing pH is slight.

One would expect that the charged nature of HMS would introduce "permselectivity" (13), resulting in the transference number of the coion (Cl^-) being significantly less than the corresponding value in aqueous solution—the effect being larger the lower the external electrolyte concentration [i.e., see Eqs. (21) and (22) in Ref. 1]. The data (Fig. 9) indicate that t_- in HMS are very close to the aqueous solution values between pH 4 and pH 8. At higher pH, significant permselectivity is evident with the expected concentration effect. At very low pH, t_- in HMS become significantly *larger* than the corresponding solution values, suggesting that the pores carry a significant positive charge below ≈pH 3. Even at pH 4, the transference number data suggest that the pores are slightly positively charged (t_- in HMS slightly higher than t_- in solution). Assuming that all pores are essentially equivalent in charge density, an analysis of the transference number data at pH 8.3 (1) gives a very small charge density (0.013 *M*) for HMS. Although the interpolation line in Fig. 9 suggests a continuous decrease for t_- in HMS between pH 5.8 and pH 8.3, with due consideration of experimental error, the data are consistent with a constant charge density of 0.013 *M* and a constant transference number over this pH range. Although a very low charge density is consistent with the volume flow data if the pore radius is very large (70 Å), other data (14) indicate that the pore radius must be less than about 25 Å. Moreover, the observation that t_- at pH 4 is greater in HMS than in solution indicates positively charged pores, which is *not* consistent with a positive J_v at pH 3.8. Thus, the transference number and J_v data appear to be mutually inconsistent. One might argue that the inconsistency has its origin in the fact that J_v is measured at high current densities, and the EMF transference numbers are measured at essentially zero current. That is, a high current density changes pore charge. However, transference numbers measured by the Hittorf method, which employs high current density, are in agreement with those measured by the EMF method, so we must look elsewhere for an explanation. The argument used to evaluate pore charge from the membrane:solution transference number difference assumes that the ratio of the coion to counterion mobility is the same in the membrane as in aqueous solution. Failure of this assumption could be the source of the anomaly. However, the Cl^--to-Na^+ mobility ratio in "low"-charge density (1.8 Eq/kg H_2O) cation-exchange resins (15) is actually slightly less than the ratio in aqueous solution and becomes larger than the aqueous solution ratio only at higher charge densities. Thus, we suspect that the source of the above anomaly lies elsewhere. We postulate that not all pores have the same size, and the charge density varies as the pore size varies. That is, the larger pores, which have a greater relative contribution to volume flow due to the dependence of L_{ve} on the square of the pore radius (1), have a greater concentration of negative charges than small pores. Thus, volume flow reflects the charge in larger pores to a much greater extent than does the transference number. This pore heterogeneity concept is developed quantitatively elsewhere (1).

Under comparable conditions, J_v for HMS is significantly less than J_v for excised human skin (5), a result in accord with a lower net concentration of negative charge in HMS pores (1). However, volume flow is still capable of transporting on the order of 0.2 mg/hr cm^2 of neutral solute from a donor solution of 20 mg/ml, provided the solute moves with the solvent. The apparent larger NaCl dependence of J_v in HMS is also in qualitative agreement with theory.

Electroosmotic flow in HMS is significantly lower at pH 3.8 than at the higher pH's. The initial J_v data (Fig. 6) show this tendency, but even more striking, the average J_v over an iontophoresis run of several hours will be essentially zero or negative at pH 3.8 because of the strong time dependence at this pH (Table I), whereas the average J_v at higher pH will be ≈8 μl hr^{-1} cm^{-2} (pH 5.8–8.3, 0.05 *M* NaCl). Similar observations were made by Rein for human skin (5). Burnette and Marrero (16) measured higher anodic iontophoretic flux of a neutral peptide at pH 8 than for the positively charged peptide at pH 4. Their interpretation of this apparent anomaly postulated greater volume flow at the higher pH, a postulate qualitatively in accord with our J_v data.

Consistent with theory (1), J_v is roughly proportional to current density and decreases sharply as the concentration of NaCl increases. A modest decrease in J_v with time is also expected when the time dependence in electrical resistance is recognized. That is, the time dependence in J_v at neutral pH (Table I) reflects, at least in part, the decreasing resistance (Fig. 3) and resulting decreasing driving force for volume flow, $-\Delta\Phi$. Changes in membrane properties may also be responsible for some of the decrease in J_v. Note that, while not statistically significant, the observed relative decrease in J_v with time is somewhat greater than the corresponding relative decrease in resistance. Some observations which appear to be beyond the scope of any simple theory are as follows. (a) J_v with the dermis side exposed to the anode is always significantly larger than when the stratum corneum is exposed to the anode. We have no explanation for this effect. (b) Significant changes in membrane properties occur when HMS is exposed to an electric field, *particularly at low pH*. The J_v data suggest that, at low pH, some negatively charged species are being extracted from the "pores," which has the effect of changing the charge concentration and, in extreme cases, removes enough material to form holes in the skin. As noted by Burnette and coworkers (17,18), electrical properties of the skin also indicate that changes in membrane properties occur as current is passed. The DC electrical resistance decreases with time, and Ohm's law is not rigorously obeyed in that the resistance decreases with increasing current density (Figs. 3 and 4). Since the conductance of the skin (reciprocal of resistance) is due to transport of small ions such as Na^+ and Cl^-, an increase in conductance (decrease in resistance) suggests that either existing "pores" are increased in size (18) or new "pores" are formed. In either case, permeability of the excised skin has been increased, much of the increase being irreversible (17).

In summary, both transference number and volume flow

data indicate that HMS carries a new negative charge at neutral and alkaline pH and becomes positively charged at low pH. Heterogeneity in pore charge appears necessary for both the transference number and the volume flow data to be fully consistent with theory. Due to a smaller net negative charge concentration, volume flow is less than in human skin but is still capable of transporting significant quantities of a neutral solute if the solute moves with the solvent. While most features of the volume flow data are consistent with simple theory (1), HMS is obviously a complex electrokinetic system which is capable of significant changes when subjected to an electric field.

REFERENCES

1. M. J. Pikal. *Pharm. Res.* 7:118–126 (1990).
2. D. G. Miller. *Chem. Rev.* 60:15–37 (1960).
3. N. Lakshminarayanaiah. *Chem. Rev.* 65:491–565 (1965).
4. Y. Kobatake, M. Yuasa, and H. Fujita. *J. Phys. Chem.* 72:1752–1757 (1968).
5. H. Rein. *Z. Biol.* 81:125–140 (1924).
6. D. J. Ives and G. J. Janz. *Reference Electrodes,* Academic Press, New York, 1961, Chap. 4.
7. H. E. Gunning and A. R. Gordon. *J. Chem. Phys.* 10:126–131 (1942).
8. M. Spiro. Determination of transference numbers. In A. Weissberger (ed.), *Physical Methods of Organic Chemistry, Part IV,* 3rd ed, Interscience, New York, 1960, pp. 3049–3111.
9. G. Scatchard. *J. Am. Chem. Soc.* 75:2883–2887 (1953).
10. R. A. Robinson and R. H. Stokes, *Electrolyte Solutions,* 2nd ed, Academic Press, New York, 1959.
11. M. J. Pikal and D. G. Miller. *J. Phys. Chem.* 74:1337–1344 (1970).
12. D. G. Miller. *J. Phys. Chem.* 70:2639–2659 (1966).
13. R. Burnette and B. Ongpipattanakul. *J. Pharm. Sci.* 76:765–773 (1987).
14. M. J. Pikal and S. Shah. *Pharm. Res.* 7:222–229 (1990).
15. M. J. Pikal and G. E. Boyd. *J. Phys. Chem.* 77:2918–2924 (1973).
16. R. Burnette and D. Marrero. *J. Pharm. Sci.* 75:738–743 (1986).
17. R. R. Burnette and B. Ongpipattanakul. *J. Pharm. Sci.* 77:132–137 (1988).
18. R. R. Burnette and T. M. Bagniefski. *J. Pharm. Sci.* 77:492–497 (1988).